Microelectronics Reliability 168 (2025) 115723

Contents lists available at ScienceDirect

Microelectronics Reliability

journal homepage: www.elsevier.com/locate/microrel

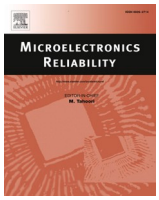

Research Paper

The behaviour of 350 V GaN HEMTs during heavy ion irradiations☆

F. Velardi [a,*], G. Canale Parola [a], S. Palazzo [a], E. Martano [a], A. Sanseverino [a], L. Silvestrin [b], C. Abbate [c], G. Busatto [a]

[a] Department of Electrical and Information Engineering, University of Cassino, Cassino, FR, Italy
[b] Dipartimento di Fisica e Astronomia, Università di Padova - INFN Sezione di Padova, Padova, PD, Italy
[c] DAC Engineering and Research srl., Via San Giovanni Battista, 2, Pontecorvo, FR, Italy

ARTICLE INFO

Keywords:
GaN HEMTS reliability
Radiation reliability
Single event burnout

ABSTRACT

The behaviour of a 350 V Enhancement Mode GaN power HEMT during heavy ion irradiation is presented. A new experimental setup has been developed to increase the sensitivity of the measurement. It allowed the measurement of the charge collected at the terminals following the impact with energetic particles to be extended by almost an order of magnitude. The results obtained, interpreted with the help of two-dimensional finite element simulations, demonstrate that the tested devices exhibit very different behaviour from those previously characterized. They do not show significant charge amplification and are not subjected to single-event gate rupture. Furthermore, it is demonstrated that the device failure is due to a recursive mechanism like that which develops in silicon PiN diodes when exposed to heavy ion irradiation.

1. Introduction

The use of enhancement mode GaN power HEMTs is becoming increasingly widespread in various areas of power electronics, including the avionics and aerospace sectors, thanks to the superior performance they guarantee in terms of conduction voltage drops and energy dissipated during switching [1]. Due to the surface structure of these devices, the absence of gate oxide, and the small sensitive volumes, these devices are expected to provide better performance in terms of tolerance to ionizing radiation compared to silicon power MOSFETs [2]. However, several studies reported in the literature [3–10] have demonstrated that enhancement mode GaN power HEMTs with blocking voltages >100 V suffer from both Single Event Burnout, SEB, and Single Event Gate Rupture, SEGR, when subjected to heavy ion irradiation.

Moreover, a significant charge amplification phenomenon is observed in these devices [4,5], which was invoked to be one of the causes of the device failure as it was shown in [11], where 2D Fine Element Simulations were used to study the failure mechanisms induced by heavy ions in enhancement mode GaN power HEMTs.

Given the surface structure and the rapid evolution of GaN technology, the performance of GaN power HEMTs, those relating to tolerance to ionizing radiation, depends significantly on the manufacturer and changes rapidly over time following the evolution of technology. Radiation reliability requires continuous updating of experimental data relating to the behaviour of such devices subjected to ionizing radiation.

This work presents the behaviour of a 350 V Enhancement Mode GaN power HEMT during heavy ion irradiation.

A new experimental setup has been developed to increase the sensitivity of the measurement. It allowed the measurement of the charge collected at the terminals following the impact with energetic particles to be extended by almost one order of magnitude. All tested HEMTs showed a permanent failure at about a fifth of the nominal blocking voltage guaranteed by the manufacturer; unlike previous devices, they did not exhibit a charge amplification mechanism and were not susceptible to gate structure damage.

The results were interpreted using two-dimensional finite element simulations, confirming that the tested devices' behaviour differs significantly from those previously characterized, particularly in charge amplification. The simulations reinforce that a bipolar mechanism is absent and that a double injection phenomenon leads to thermal failure.

2. The experiment setup

Due to the very low sensitivity volume associated with energetic particle impacts in power GaN HEMTs, the charge collected at the terminals is very low, and the amplitude of the current pulses acquired

☆ This article is part of a Special issue entitled: 'ESREF 2024' published in Microelectronics Reliability.

* Corresponding author at: Dept. of Electrical and Information Engineering, University of Cassino, Via G. Di Biasio, 43, 03043 Cassino, FR, Italy.
E-mail address: velardi@unicas.it (F. Velardi).

https://doi.org/10.1016/j.microrel.2025.115723
Received 22 November 2024; Received in revised form 13 February 2025; Accepted 24 March 2025
Available online 1 April 2025

during irradiation is very small. This is especially true for state-of-the-art devices where no significant charge amplification phenomena are evident, as will be demonstrated below. This required the development of a new measurement apparatus with higher sensitivity and signal-to-noise ratio.

The schematic of the developed circuit is depicted in Fig. 1. The experimental circuit and procedure agree with method 1080 of the military standard 750 for SEB/SEGR characterization.

The setup is based on the circuit described in [12], which was modified to include wide bandwidth amplifiers (BW > 1 GHz) in both the drain and gate signal branches. The new layout enhances the measurement system's sensitivity, allowing us to detect lower collected charges more efficiently.

The amplifier schematic is shown in Fig. 2. It was designed to be a little board, see Fig. 3, to be inserted on the main board, as shown in Fig. 4.

The amplifier's core is a Monolithic Microwave Integrated Circuit (MMIC), a small IC able to operate up to microwave frequencies. A suitable MMIC for our application was chosen by comparing the performance of different commercial devices, considering factors such as bandwidth, gain, and noise figures. The chosen MMIC is an AGB3303 manufactured by ANADIGICS. This surface-mount InGaP Heterojunction Bipolar Transistor amplifier ensures high flat gain and low noise figure at our operating frequencies due to its elevated input third-order intercept point (IP3). Additionally, its inherent feedback circuit provides unconditional stability.

To transfer maximum power through the amplifier and minimize noise-causing reflections, its input and output impedance were set to 50 Ω. Additionally, 50 Ω connection lines were used between the amplifier and the BNC connector to the oscilloscope. Considering the thickness and average dielectric constant of the FR4 substrate, along with the height and length of the PCB copper track, we determined the optimal width of the microstrip needed to match a 50 Ω impedance at a frequency of 1 GHz.

The AGB3303 requires a single-voltage supply; the voltage is applied through the bias resistor R and the inductor L1 + L2 at the output terminal, and the filter capacitors, C3 and C4, prevent high-frequency signals from reaching the voltage supply, see Fig. 2.

The amplifier is optimized for a bias current of 80 mA; using an +8 V supply, a resistor value of 38 Ω provides an appropriate bias current.

To enhance its self-resonant frequency and not degrade the amplifier's bandwidth, the high-value filter inductor has been effectively divided into a series comprising a high-value inductor, L_2, and a low-value inductor, L_1. This strategic split ensures a high inductance value with a small parasitic capacitance value.

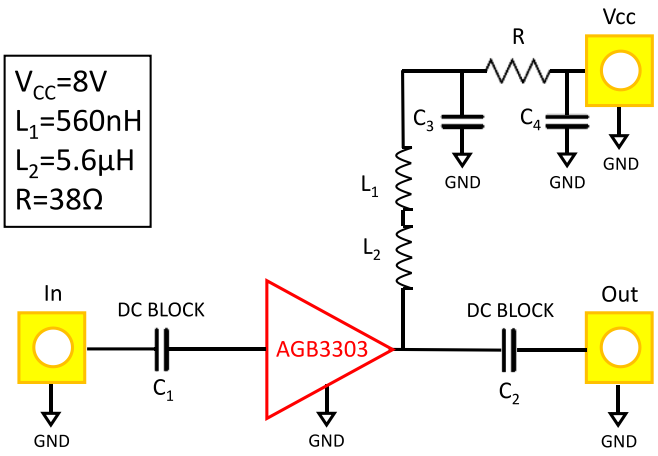

Fig. 2. Schematic of the amplification board.

Dually, the DC blocking capacitors, C_1 and C_2, were constructed by paralleling two high-value capacitors. This configuration was chosen to achieve a substantial total capacitance while minimizing stray inductance.

3. The experimental results

Commercial Enhancement Mode GaN Power HEMTs rated at 350 V–6.3 A were irradiated at the SIRAD facility of the Laboratori Nazionali di Legnaro, INFN, Italy [13]. The devices were exposed to ^{107}Ag ions at 228 MeV with a flux of about 2 k ions cm^{-2} s^{-1}, corresponding to an ion impact frequency of about 80 ions per second on the DUT surface. This low frequency ensures a low probability of having two ion impacts in each oscilloscope acquisition window to simplify statistical analysis performed after irradiation. The duration of the total irradiation on a single device was fixed to have statistically significant event populations and, at the same time to avoid dose effects.

The silver energy loss and penetration range were evaluated using the Stopping and Range of Ions in Matter (SRIM) software [14]. The SRIM simulations were conducted on a multilayer sequence that replicates the vertical structure of the tested GaN HEMT. Fig. 5 shows the calculated LET for the considered silver ion. The ion traverses all GaN

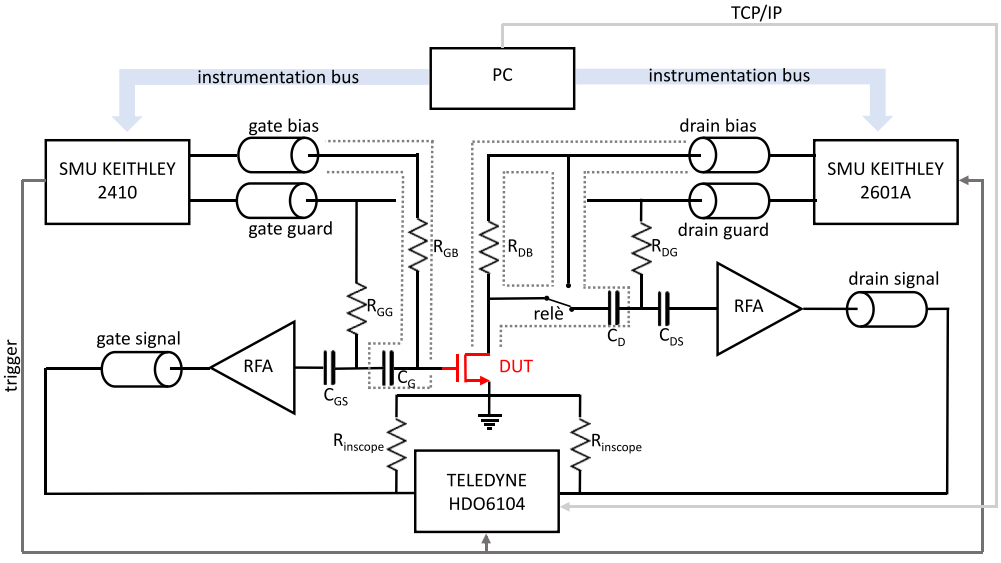

Fig. 1. Schematic of the test board.

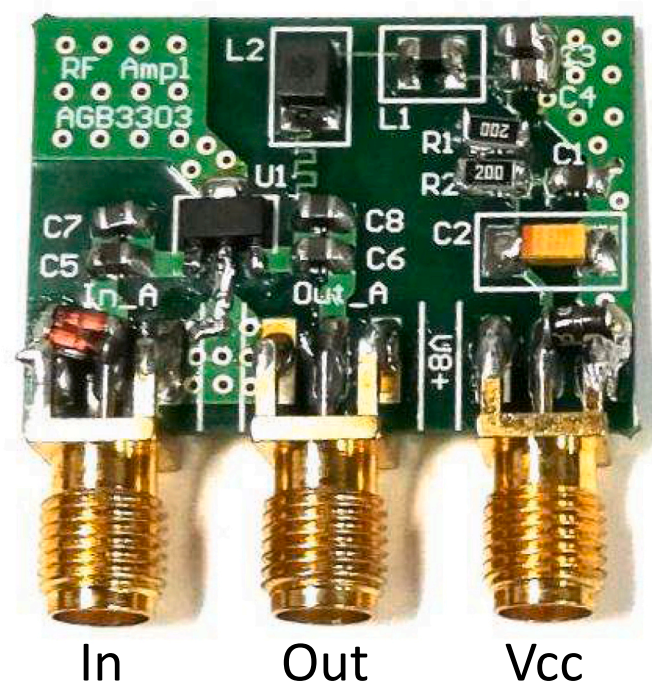

Fig. 3. Picture of the amplification board.

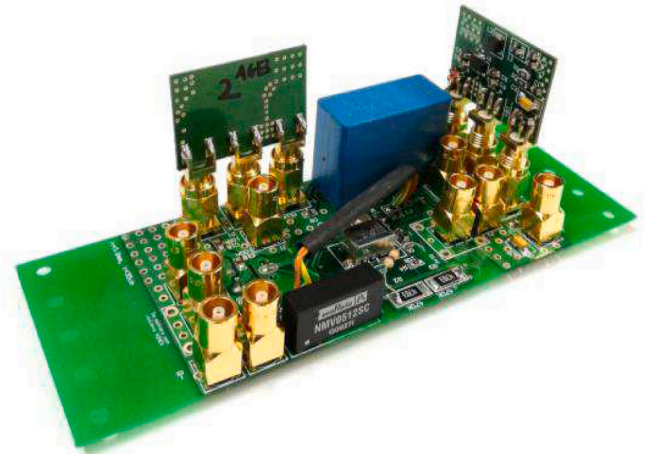

Fig. 4. Picture of the test board with the amplifiers.

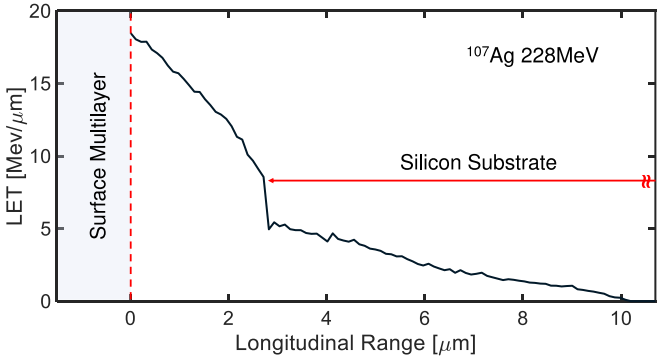

Fig. 5. The simulated LET for ^{107}Ag ions at 228 MeV.

and AlGaN regions, the AlN nucleation layer, and stops in the silicon substrate, releasing a charge of approximately 1 pC in the semiconductor layers.

The HEMT under test was reverse biased with a fixed drain voltage during each irradiation step. Both gate and drain leakage currents were continuously monitored. A fast-digitizing oscilloscope captured the current pulses associated with the charge generated during each ion impact and collected at drain and gate terminals. We electrically characterized the device to identify potential structural damage after each irradiation step. If no damage was detected, we proceeded with a new irradiation step using a higher drain bias voltage. The experimental procedure is detailed in reference [12].

All tested devices exhibited a permanent failure at about $V_{DB} = 75$ V, almost a fifth of the nominal DUT blocking voltage guaranteed by the manufacturer.

Figs. 6 and 7 report the time evolution of the drain and gate leakage current during irradiation at the critical bias voltage, respectively.

The device under test fails after approximately 50 s when the drain leakage current abruptly reaches its compliance value. The massive increase in drain current is only minimally reflected at the gate terminal; after a jump of just 4 μA, the gate leakage current drops off very slowly. Looking at the two figures, it can be deduced that the burnout concerns the drain area and does not affect the gate structure. The post-irradiation electrical characterization confirms this statement, as shown in Fig. 8, which compares the gate leakage current measured before and after irradiation at the critical bias voltage. The two curves' perfect overlap excludes the gate structure's damage.

By method 1080 of military standard 750, the low flow ensures that the rupture is not due to an accumulated dose effect. As a verification, a pristine device was irradiated directly at $V_{DB} = 75$ V, showing a similar failure. Fig. 9 compares the time evolution of drain current during silver irradiation at $V_{DB} = 75$ V for a pristine device (black curve) and a pre-irradiated device (red curve). Despite starting from very different initial conditions, a few nanoamperes for the pristine device and tens of microamperes for the pre-irradiated device, both drain currents show the same prompt growth rate, indicating the occurrence of rupture.

The red waveform in Fig. 10 shows the SEB drain current pulse measured at the DUT failure, i.e., the current pulse detected at the drain terminal corresponding to the current fast increase; the curve is clipped due to the inadequate scale of the oscilloscope. To better understand the proportion of the pulse and the speed of its rising edge, the SEB waveform is also compared to a typical pulse recorded during the same irradiation step (black curve).

The charge of the current pulses detected during each irradiation step was evaluated and statistically analyzed over a population of at least 150 events. Fig. 11 depicts the average and maximum charge values associated with the current pulses detected during the irradiation at increasing drain bias starting from $V_{DB} = 50$ V with steps of 5 V until DUT failure. The mean value of the charge is practically constant around 2 pC, and the maximum measured charge never exceeds 8 pC, even at biasing conditions near the SEB voltage. These charges are close to the value of about 1 pC deposited by the impacting particle. This charge is much smaller than that measured on previous generation GaN HEMTs for which much larger charges have been measured at voltages near the SEB occurrence. For comparison, the mean charge measured in [5] during irradiation of GaN HEMTs (EPC 2015 and 1007) in similar irradiation conditions is reported in Fig. 12. The charge measured on these latter devices is a few nanocoulombs, that is almost three orders of magnitude larger than that measured in the new generation devices (see Fig. 11).

The above results indicate that the new generation devices are not affected by charge amplification mechanisms which was observed in the devices previously tested, and which was attributed to a bipolar effect initiated by the surviving holes after the ion impact, forming the base of a parasitic bipolar transistor which can cause DUT SEB [5].

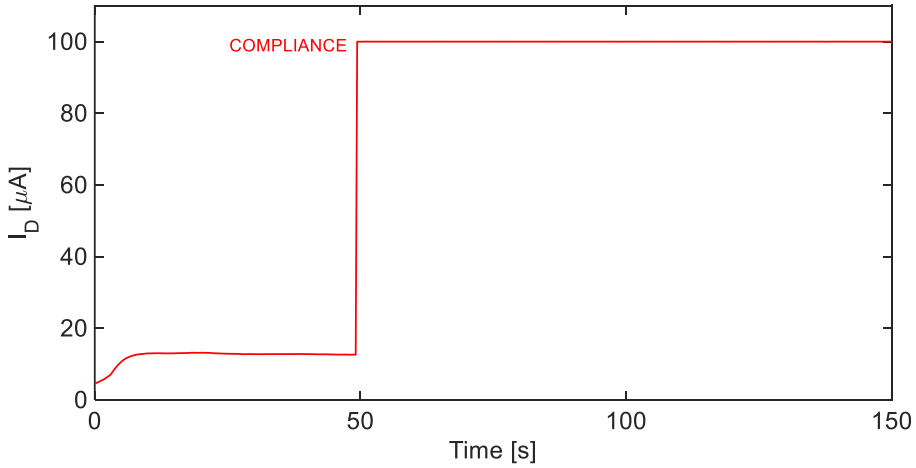

Fig. 6. Drain leakage current during irradiation with ^{107}Ag @ 228 MeV, V_{DB} = 75 V.

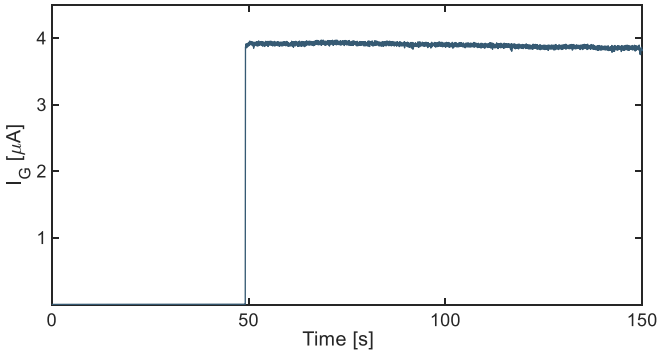

Fig. 7. Gate leakage current during irradiation with ^{107}Ag @ 228 MeV, V_{DB} = 75 V.

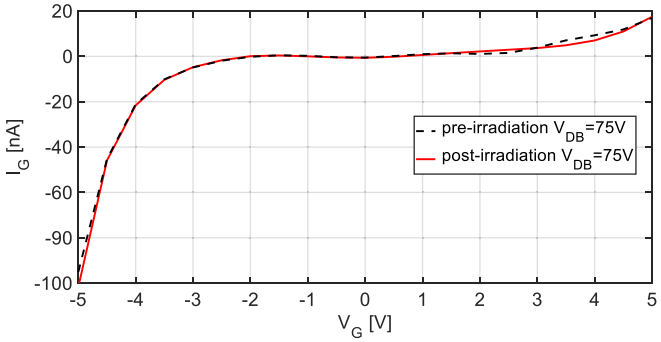

Fig. 8. Gate electrical characterization after and before irradiation with ^{107}Ag @ 228 MeV, V_{DB} = 75 V.

4. Simulation results and discussion

The experimental results were interpreted using 2D thermoelectrical finite element simulations performed using TCAD tools from Synopsys [15]. The parameters used to obtain the GaN HEMT elementary cell were extrapolated from the literature [16] and modified to better reproduce the tested device's behaviour. Fig. 13 shows the satisfying overlap between the breakdown characteristic of the device obtained experimentally (black curve) and by simulation (red curve).

Particular care was dedicated to the model of the charge deposition in the device associated with the impact of the energetic particle. The SRIM program determined the amount of ionization energy released

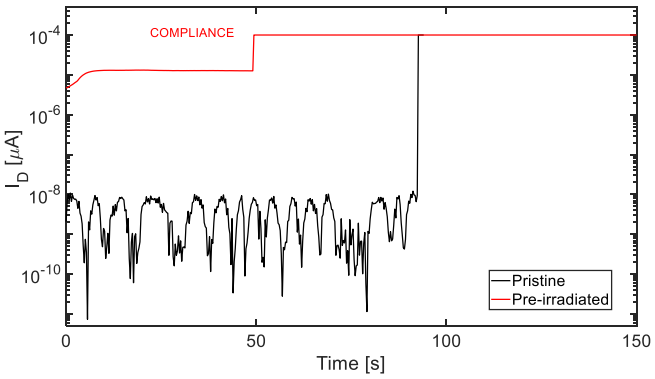

Fig. 9. Comparison of drain leakage currents during irradiation with ^{107}Ag @ 228 MeV, V_{DB} = 75 V, among pristine and pre-irradiated devices.

along the silver ion track. Subsequently, this transferred energy was discretized with a step of 0.01 μm and converted to equivalent electron-hole pairs. We consider an exponential decrease in generated charge along the radius perpendicular to the ion trajectory and a Gaussian decay over time that begins with the entry of the silver ion.

A sketch of the simulated device is shown in the upper part of Fig. 14, where four selected significant impact points are highlighted, namely:

a) the right edge of the source terminal;
b) the right edge of the gate terminal;
c) the right edge of the field plate;
d) the left edge of the drain terminal.

At the bottom of the same figure, the simulated total current density distribution during silver irradiation at V_{DB} = 50 V is reported for the four impact points. The distributions refer to the instant the current pulse reaches its maximum value.

In addition, the current pulse evolution in case d) is superimposed on the related distribution.

The maximum interaction between the impacting ion and the device develops in case d). At low bias voltage values, the electric field assumes its peak near the drain terminal. When the ion impacts in this region, the charge generated due to its transit induces an intense plasma filament which increases the electric field beyond its original distribution; this increased electric field promotes a rapid charge collection by drift, clearly visible in the first sudden peak of the current pulse.

As the electric field resumes its initial distribution, a carrier diffusion dominates the charge collection. This diffusion is responsible for the

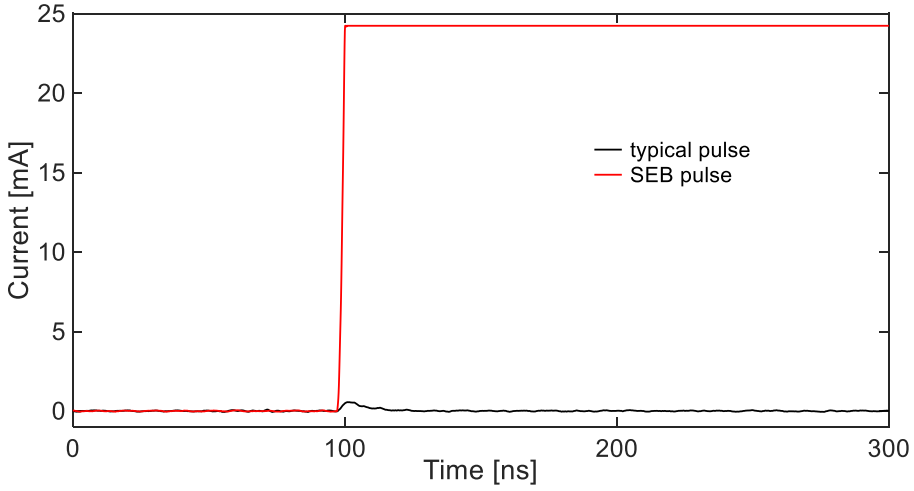

Fig. 10. Comparison between the SEB and a typical drain current pulse in the same bias condition.

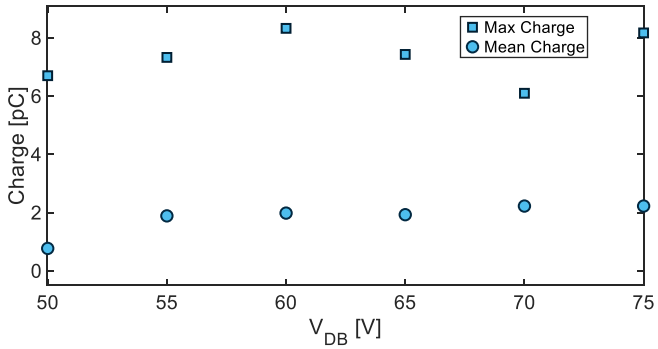

Fig. 11. Mean and maximum value of the collected charge.

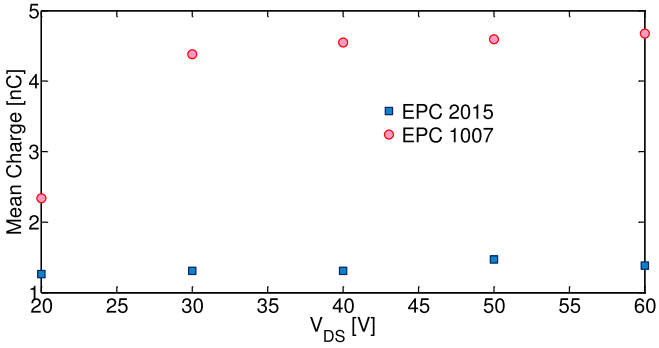

Fig. 12. Mean value of the collected charge [15].

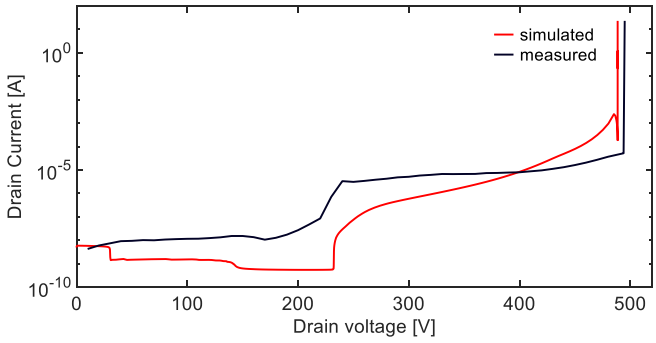

Fig. 13. The BV characteristic of the simulated device, red curve, and the tested device, black curve. (For interpretation of the references to color in this figure legend, the reader is referred to the web version of this article.)

extended evolution of the current pulse. Fig. 14.d) shows how the current is distributed between the drain and body, and no relevant component flows through the source and gate terminals. The collected charge between about 0.5 pC and 2 pC obtained by simulation confirms the experimental observation for which no significant amplification mechanism was evidenced, contrary to what was found in GaN devices previously investigated in the literature [4,5].

The simulation results of Fig. 14 indicate that the further away the impact point is from the drain, the less the interaction between the plasma filament and the electric field and, consequently, the less charge is collected at the external terminals. If the ion hits the field plate and the gate at the right edge, the charge is reduced to about one-third and one-quarter of the maximum value, respectively. If the ion hits the right edge of the source, the collected charge is negligible.

Fig. 15 refers to a 228 MeV silver irradiation at the critical bias voltage and ion impact at the left edge of the drain contact.

The electron-hole pairs released by the silver ion locally perturb the electric field and cause the formation of a second electric field peak at the buffer/nucleation layer interface, see Fig. 15.a). A considerable impact ionization rate occurs along the ion track at both drain/metal and buffer/nucleation layer interfaces, see Fig. 15.b).

The carriers are generated by impact ionization in these two interface regions and are accelerated by the electric field toward the plasma filament: electrons from the surface interface and holes from the bottom one. These carriers replace the electron-hole pairs which recombine in the plasma filament. The high values of the electric field and the related impact ionization rate are sustained by the external biasing voltage.

In such way, a self-sustaining and stable mechanism is originated, and a considerable current density rapidly develops between drain and body, leading to a thermal burnout. This failure mechanism is analogous to that which develops in silicon PiN diodes subjected to heavy ion irradiation [17].

The thermal map of the elementary cell reported in Fig. 15.c) shows a substantial temperature increase at both interfaces. For clarity, zoom around the drain metal contact is provided in Fig. 15.d); the temperature exceeds a value of 1000 K, recognized in the literature as the threshold for causing device failure by thermal degradation of the metal contact [18,19].

Fig. 16.a) shows a microscope picture of the surface of a pristine device, highlighting the metal terminals: the source (red points), drain (blue points), and gate (green point). Below, Fig. 16.b) displays the same

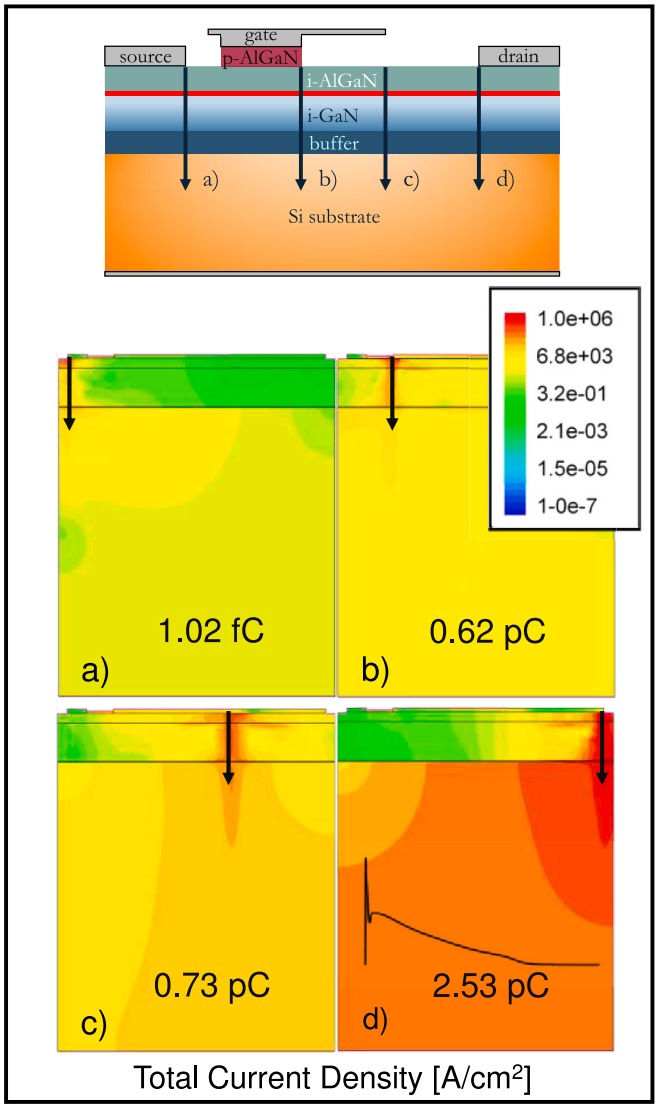

Fig. 14. Current density for Ag ion impacting at the: a) right edge of the source; b) right edge of the gate; c) right edge of the field plate; d) left edge of the drain.

device surface after silver irradiation at the critical bias voltage. Only the gate metallization is intact, while thermal-induced melting deeply damages the drain and source contacts. To understand why the source metallization is also damaged together with the drain one, let us consider Fig. 17 [20]. It shows a sketch of the device structure where the internal backside via connecting the body metallization with the external source metallization is highlighted in yellow together with the body. Due to the regenerative mechanism described above, the ion impact causes a massive current between the drain contact and the body region below it. This current is supported by the external bias voltage that is applied between the source and drain terminals. The current will therefore flow through the path of minimum resistance highlighted with a red arrow in the structure of Fig. 17. This path includes the body, the internal backside via, and the source contact, which, therefore, will be affected by the same current as the drain contact and will be damaged like it.

5. Conclusions

The behaviour of a 350 V Enhancement Mode GaN power HEMT during heavy ion irradiation has been presented. Thanks to a new experimental setup and with the help of 2D FEM simulations, it has been

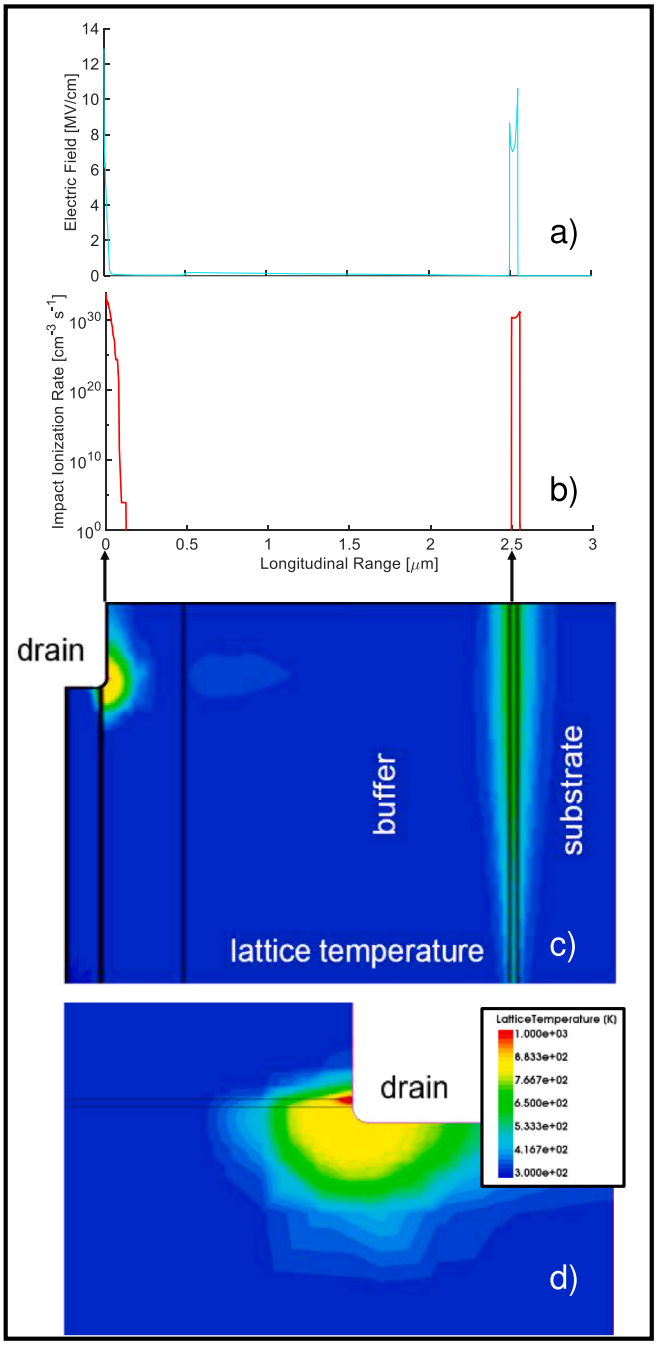

Fig. 15. Simulation results at the critical voltage for: a) Electric Field along the ion track; b) Impact Ionization Rate along the ion track; c) Thermal Map of the cell; d) zoom of the Thermal Map around the drain.

demonstrated that the tested devices exhibit a different behaviour from other devices with similar characteristics previously analyzed in the literature. They do not exhibit significant charge amplification and are not affected by single-event gate failure. Furthermore, it has been demonstrated that the failure is not attributable to a parasitic bipolar effect. The failure mechanism has been identified thanks to 2D FEM simulations and confirmed by a post irradiation failure analysis. The device failure is due to a recursive mechanism like that which develops in silicon PiN diodes when exposed to heavy ion irradiation.

Declaration of competing interest

The authors declare that they have no known competing financial

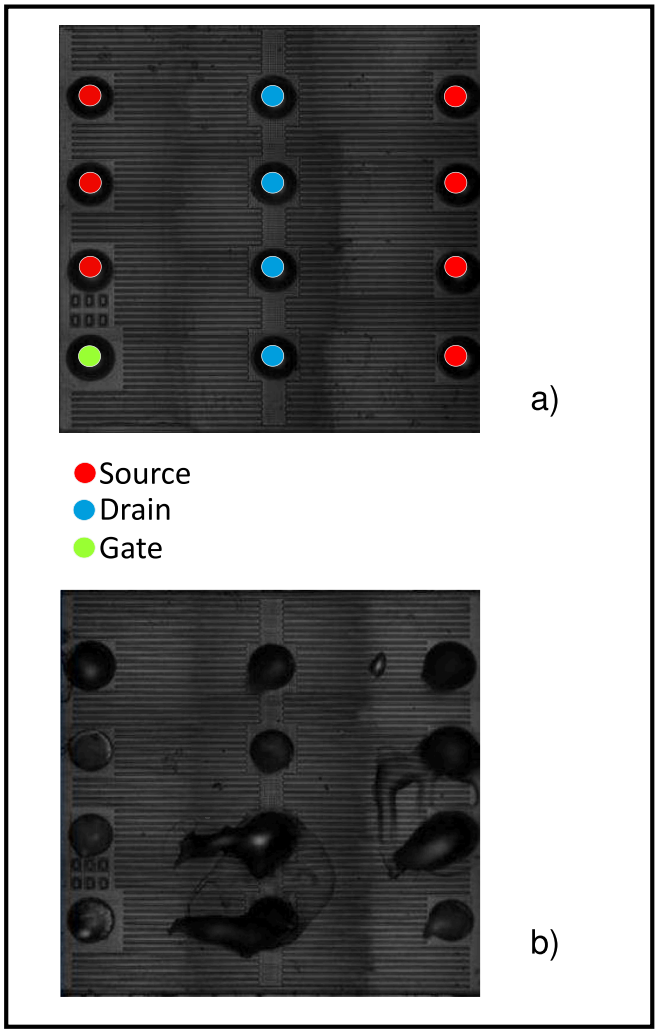

Fig. 16. View of the device surface with its terminals: a) pristine; b) after irradiation at the critical bias voltage.

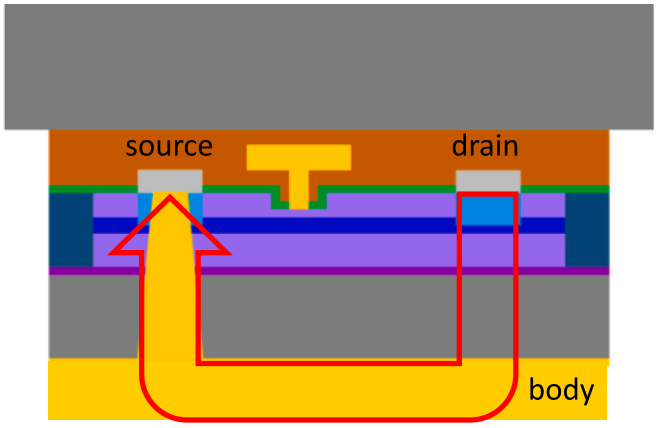

Fig. 17. Sketch of the device in which the internal backside via between body and source is highlighted [20].

interests or personal relationships that could have appeared to influence the work reported in this paper.

Acknowledgments

The authors wish to acknowledge the staff of the SIRAD irradiation facility and the staff of the TANDEM-XTU irradiation facility of the Laboratori Nazionali di Legnaro, INFN, Legnaro, for the precious support supplied during the irradiation campaigns. Moreover, the authors wish to acknowledge Dr. Davide Tedesco and Dr. Albert Scala for their contribution to constructing the test boards.

Data availability

Data will be made available on request.

References

[1] M. Carbone, et al., An overview of GaN FET …, in: 2019 European Space Power Conference (ESPC), Juan-les-Pins, France, 2019, pp. 1–4.
[2] S. Bazzoli, et al., SEE sensitivity of a COTS GaN …, in: 2007 9th European Conference on Radiation and Its Effects on Components and Systems, Deauville, France, 2007, pp. 1–5.
[3] L. Scheick, Determination of single-event effect …, IEEE Trans. Nucl. Sci. 61 (6) (Dec. 2014) 2881–2888.
[4] S. Onoda, et al., Enhanced charge collection …, IEEE Trans. Nucl. Sci. 60 (6) (Dec. 2013) 4446–4450.
[5] C. Abbate, et al., Experimental study of single event effects …, Microelectron. Reliabilty 55 (9–10) (Aug./Sep. 2015) 1496–1500.
[6] E. Mizuta, et al., Single-event damage …, IEEE Trans. Nucl. Sci. 65 (8) (Aug. 2018) 1956–1963.
[7] A.M. Zerarka, O. Crepel, Radiation robustness of normally-off …, Microelectron. Reliability 88–90 (September 2018) 984–991.
[8] Y. Wu, J. Zhang, S. Zhao, et al., Investigation of heavy ion …, Sci. China Inf. Sci. 65 (2022) 182404.
[9] D.M. Fleetwood, et al., Radiation effects in AlGaN/GaN HEMTs, IEEE Trans. Nucl. Sci. 69 (5) (May 2022) 1105–1119.
[10] M.A.J. Rasel, et al., Heavy ion irradiation …, J. Phys. D Appl. Phys. 56 (30) (2023).
[11] M. Zerarka, et al., TCAD simulation of the single event effects …, IEEE Trans. Nucl. Sci. 64 (8) (Aug. 2017) 2242–2249.
[12] C. Abbate, et al., Gate damages induced … part I, IEEE Trans. Electron Devices 66 (10) (Oct. 2019) 4235–4242.
[13] J. Wyss, et al., SIRAD: an irradiation facility at the LNL …, Nuclear Instruments and Methods in Physics Research A462 (2001) 426–434.
[14] J.F. Ziegler. "SRIM", IBM Research. SRIM - The Stopping and Range of Ions in Matter.
[15] Sentaurus TCAD Tools, Synopsis, Mountain View, CA, USA, 2013.
[16] O. Hilt, et al., Normally-off algan/gan…and algan buffer, in: 22nd ISPD, 2010, pp. 347–350.
[17] G. Soelkner, et al., Charge carrier avalanche multiplication…, IEEE Trans. Nucl. Sci. 47 (6) (2000) 2365–2372.
[18] F.B. Pribahsnik, et al., Exploring the thermal limitation…, Microelectron. Reliability 26–27 (September 2017) 304–308.
[19] D. Maier, et al., Testing the temperature limits of GaN-based HEMT devices, IEEE Transactions on Device and Material Reliability 10 (4) (December 2010) 427–436.
[20] www.ulvac.co.jp/wiki/en/process_g_gan_hemt/.